

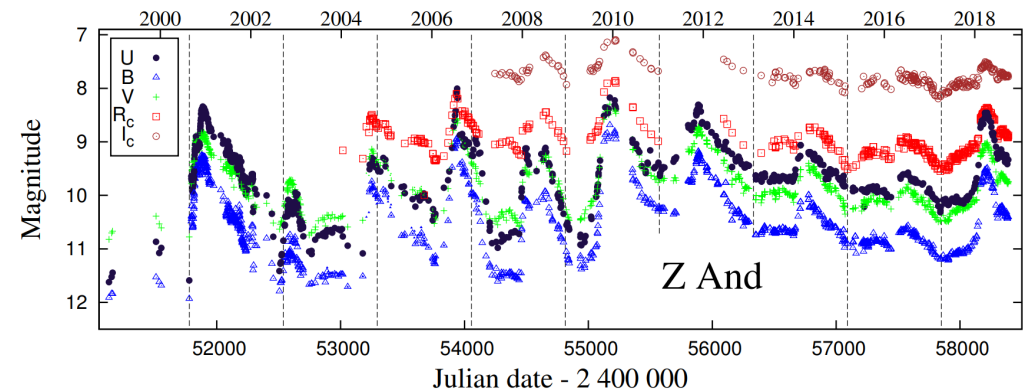
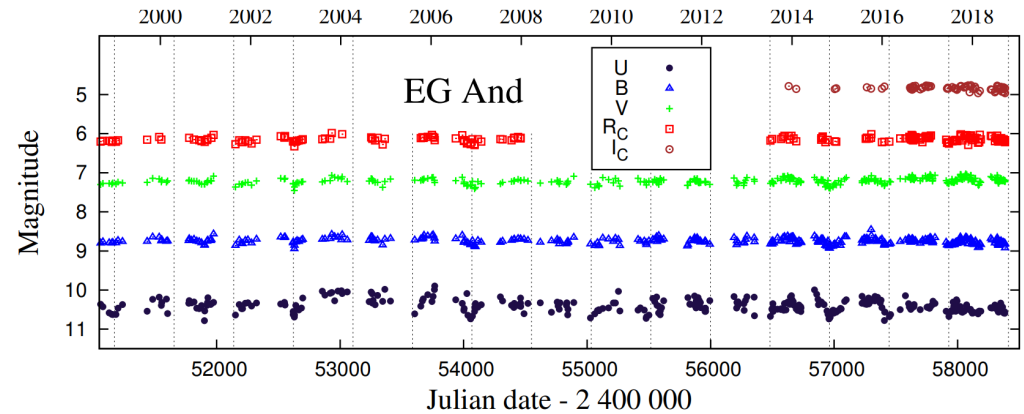
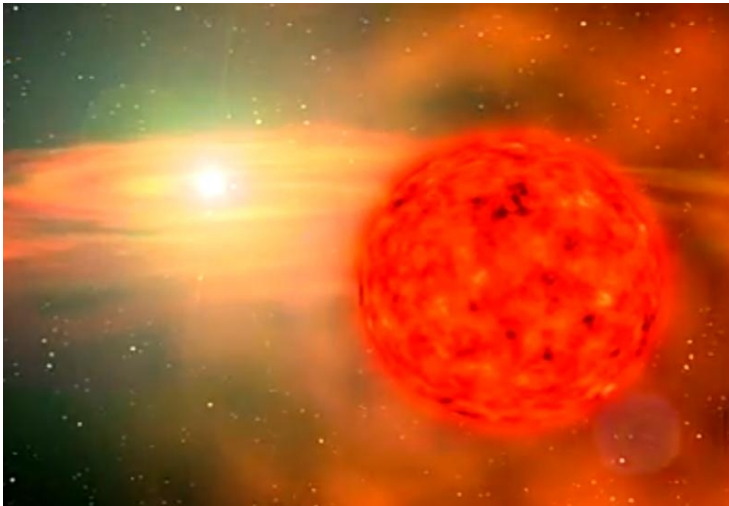
Asymmetries of the Wind from Giants *in S-type Symbiotic Binaries* **from UV and Optical Observations**

N. Shagatova and A. Skopal

Astronomical Institute, Slovak Academy of Sciences, Tatranská Lomnica, Slovakia

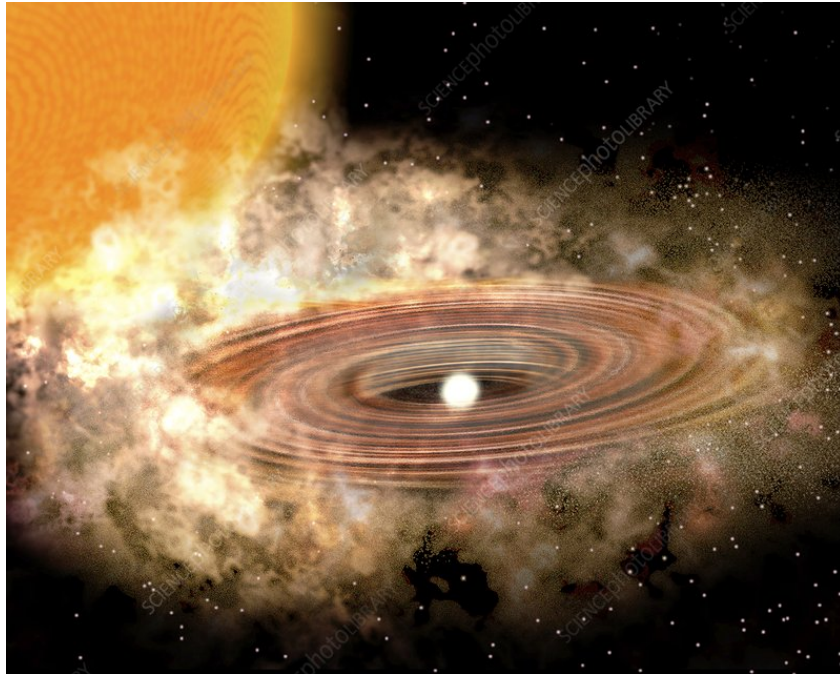
S-type symbiotic stars

- wide interacting binary stars ($P \approx$ few years)
- white dwarf + red giant (RGB)
- mass transfer via stellar wind
- neutral and ionized wind
- quiescent and active phases



The luminosity problem

- accretion heats up the white dwarf up to $T \sim 100\,000\text{ K}$ and $L \sim 1000 L_{\text{Sun}}$



Required **accretion rate** :
 $10^{-8} - 10^{-7} M_{\text{Sun}} / \text{year}$

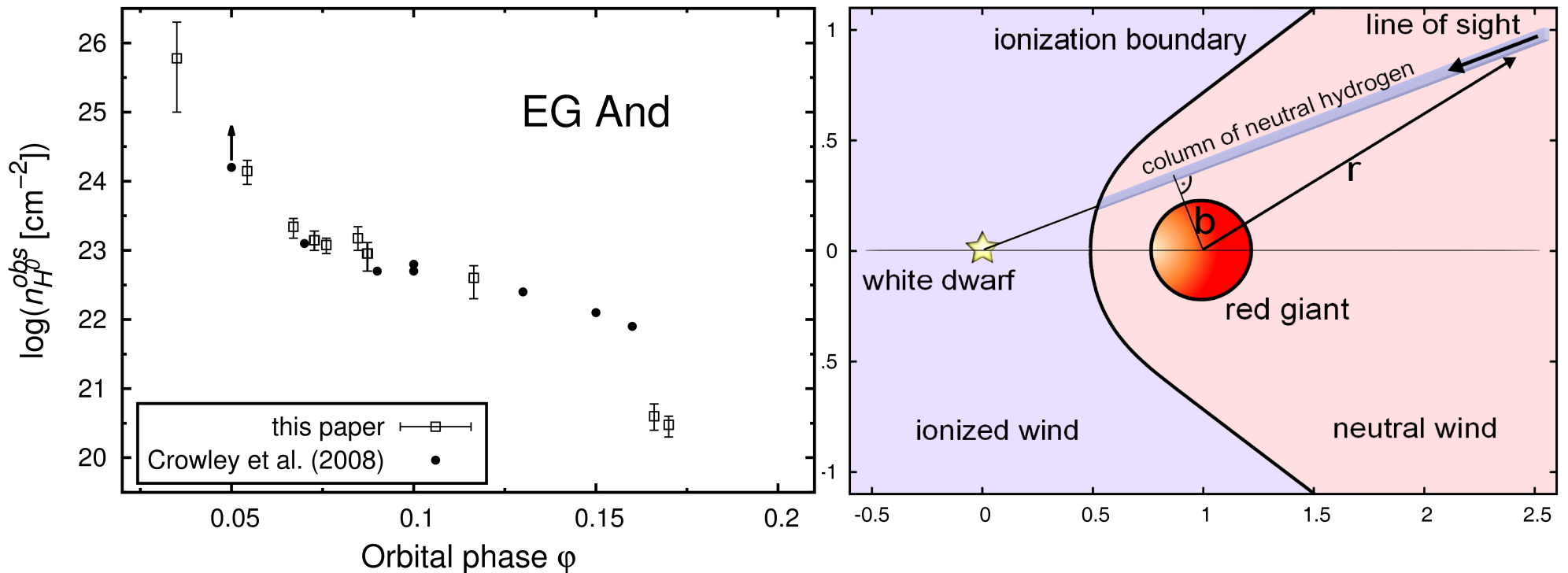


Measured **mass-loss rate** :
 $\sim 10^{-7} M_{\text{Sun}} / \text{year}$

- binary stars: mass accretion rate \sim few % of the mass loss rate

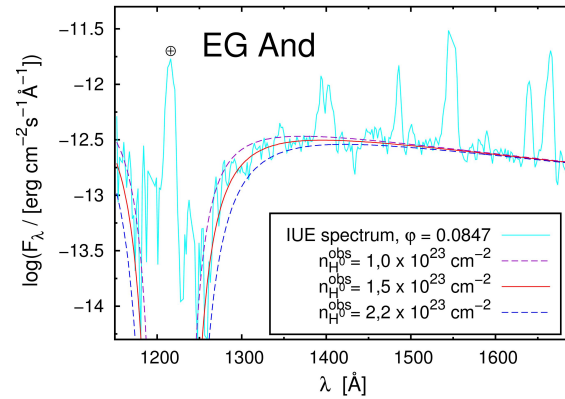
H⁰ column density during quiescent phases

- no outbursts on the white dwarf
- conical neutral wind area around the red giant
- fraction of the red giant wind ionized by the white dwarf



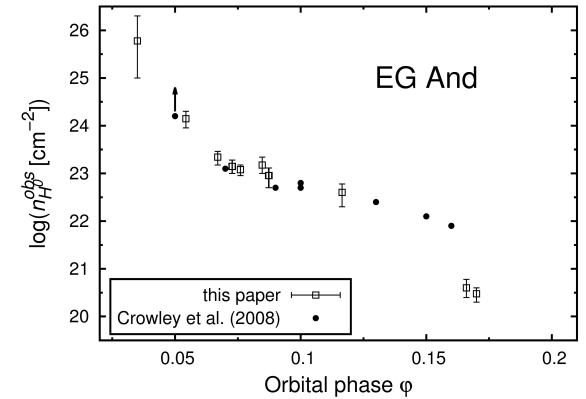
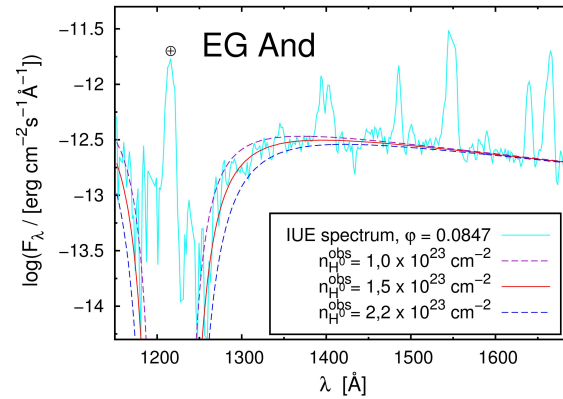
H⁰ column densities from Rayleigh scattering

- for **EG And** and **SY Mus**
- *IUE* and *HST* spectra
- + adopted values from literature



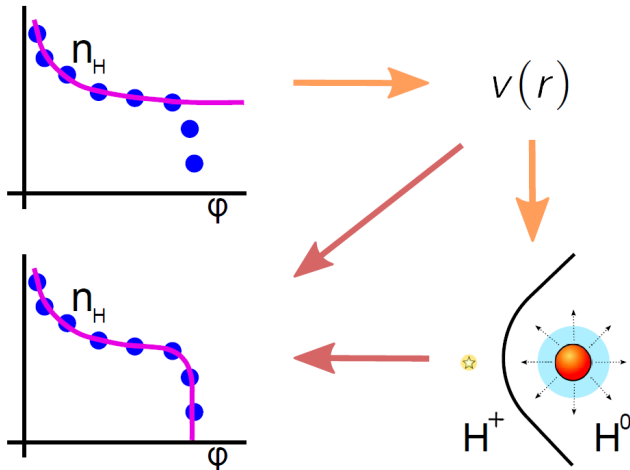
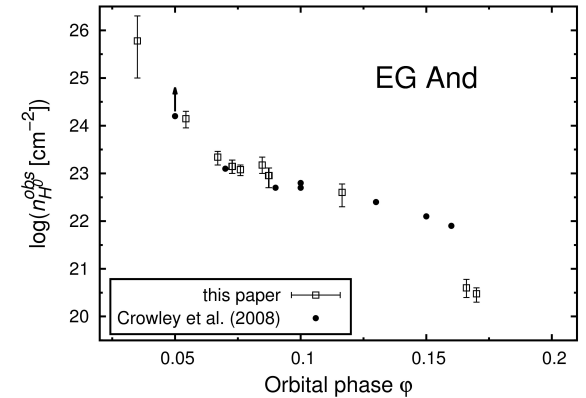
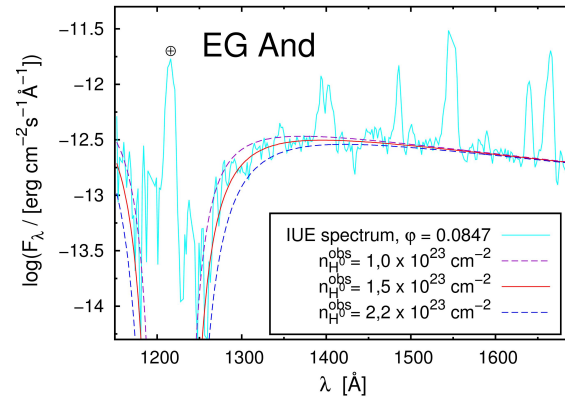
H⁰ column densities from Rayleigh scattering

- for **EG And** and **SY Mus**
- *IUE* and *HST* spectra
- + adopted values from literature



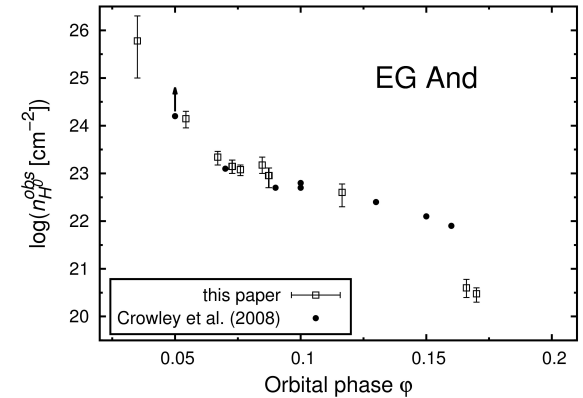
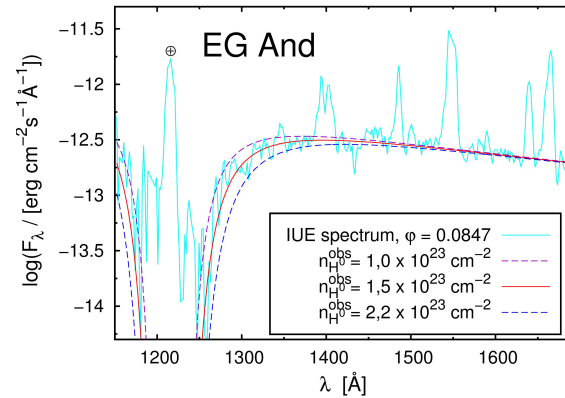
H⁰ column densities from Rayleigh scattering

- for **EG And** and **SY Mus**
- *IUE* and *HST* spectra
- + adopted values from literature

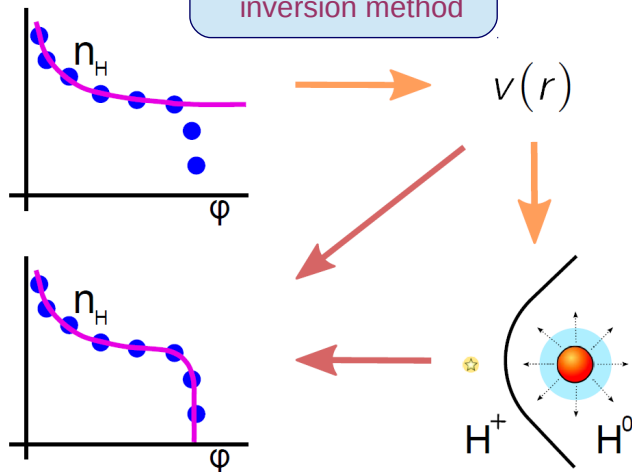


H⁰ column densities from Rayleigh scattering

- for **EG And** and **SY Mus**
- *IUE* and *HST* spectra
- + adopted values from literature

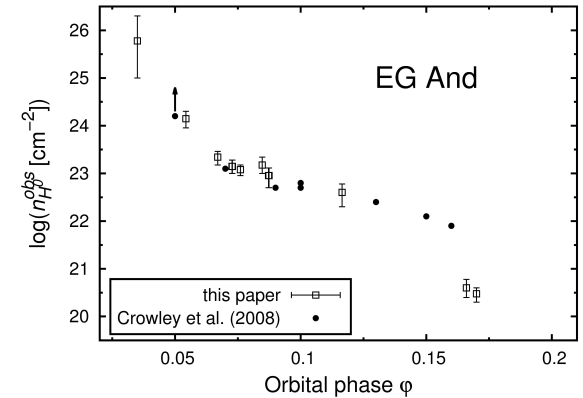
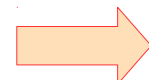
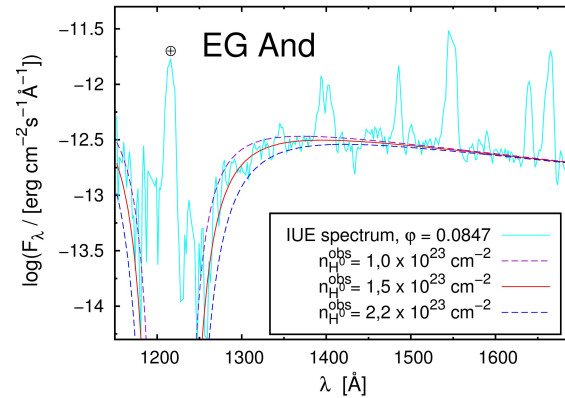


Knill et al. (1993)
A&A 274, 1002
inversion method

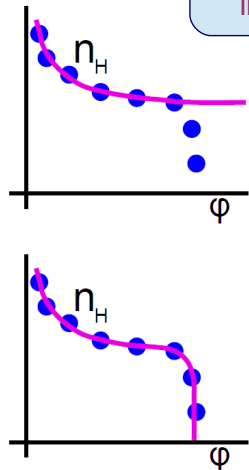


H⁰ column densities from Rayleigh scattering

- for **EG And** and **SY Mus**
- *IUE* and *HST* spectra
- + adopted values from literature

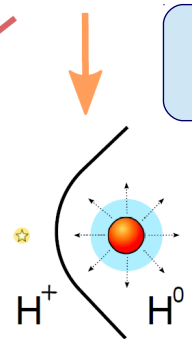


Knill et al. (1993)
A&A 274, 1002
inversion method

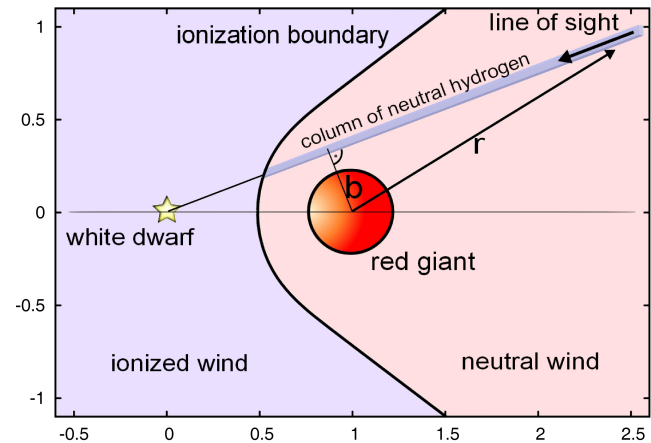


$v(r)$

Seaquist et al. (1984)
ApJ 284, 202
ionization boundary



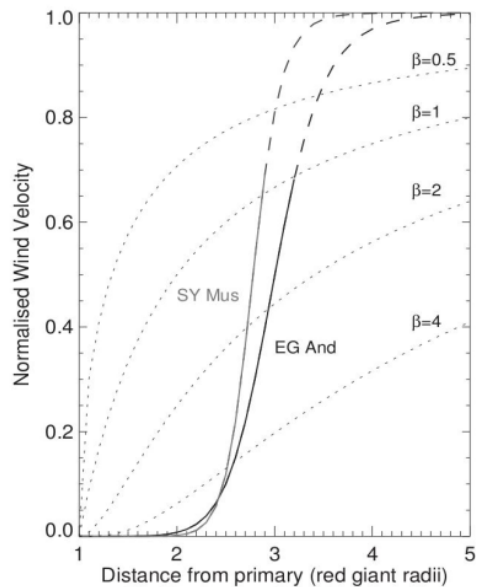
- including **ionization** of the wind



Velocity profile

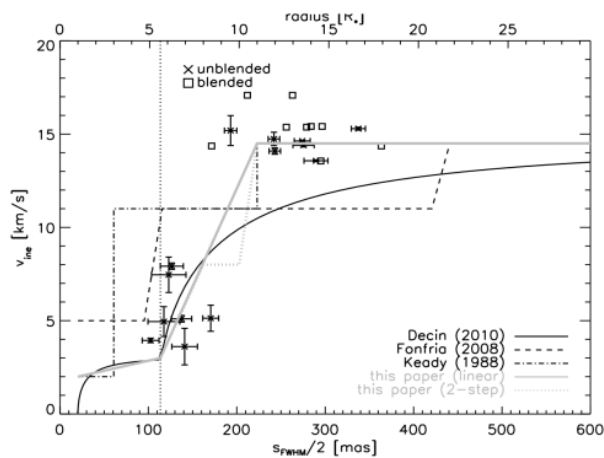
- canonical β -law

$$v(r) = v_\infty \left(1 - \frac{R}{r}\right)^\beta$$



Crowley & Espey 2010, ASP Conf. Ser. 425, 191

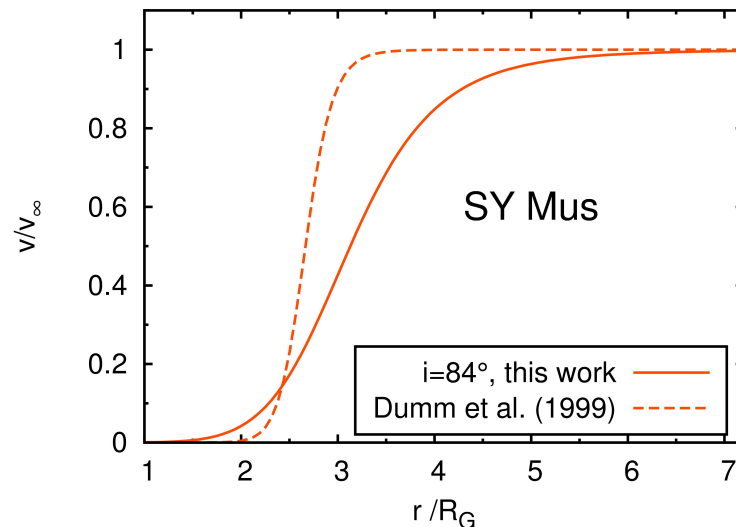
- steeper $v(r)$ for cooler stars



Decin et al. 2015, A&A 574, A5

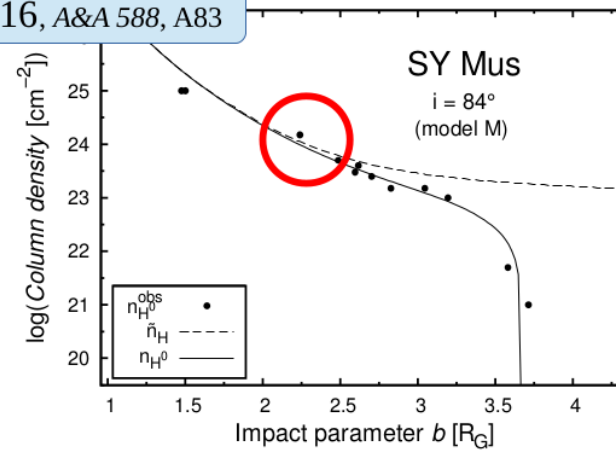
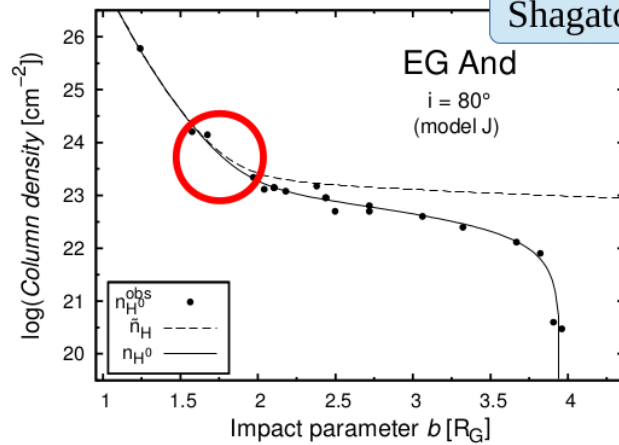
- simple analytic formula:

$$v(r) = \frac{v_\infty}{1 + \xi r^{1-K}}$$

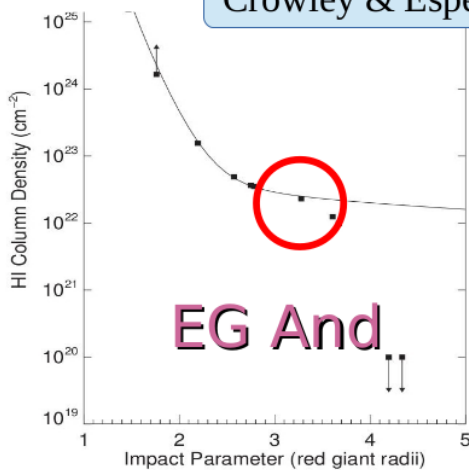


Column density models - comparison

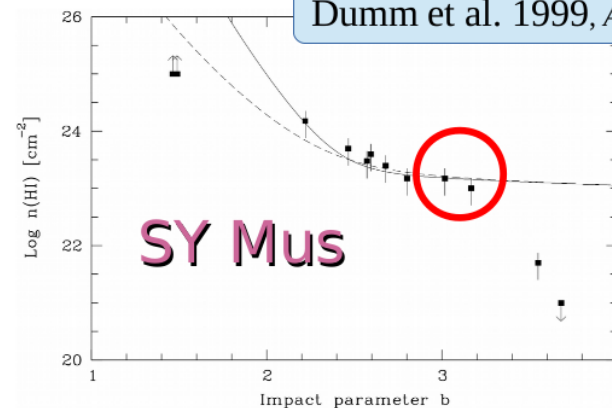
Shagatova et al. 2016, A&A 588, A83



Crowley & Espey 2010, ASP Conf. Ser. 425, 191



Dumm et al. 1999, A&A 349, 169



Wind enhancement in the orbital-plane area

Object	i	$\dot{M}_{\text{sp}} [M_{\odot} \text{yr}^{-1}]$	model
EG And	70°	1.06×10^{-6}	I
	80°	9.00×10^{-7}	J
	90°	7.91×10^{-7}	K
SY Mus	80°	2.13×10^{-6}	L
	84°	1.65×10^{-6}	M
	90°	1.62×10^{-6}	N
	84°	6.51×10^{-7}	O

Shagatova et al. 2016, A&A 588, A83

Wind enhancement in the orbital-plane area

Object	i	$\dot{M}_{sp} [M_{\odot} \text{yr}^{-1}]$	model
EG And	70°	1.06×10^{-6}	I
	80°	9.00×10^{-7}	J
	90°	7.91×10^{-7}	K
SY Mus	80°	2.13×10^{-6}	L
	84°	1.65×10^{-6}	M
	90°	1.62×10^{-6}	N
	84°	6.51×10^{-7}	O

Shagatova et al. 2016, A&A 588, A83

Mass-loss rate for giants in S-type symbiotic systems from **line-of-sight independent** methods $\approx 10^{-7} M_{\odot}/\text{year}$
(from nebular emission in radio and optical wavelengths)

Seaquist et al. 1993, ApJ 410, 260

Mikołajewska et al. 2002, Adv. Space Res. 30, 2045

Skopal 2005, A&A 440, 995

Wind enhancement in the orbital-plane area

Object	i	$\dot{M}_{sp} [M_{\odot} \text{yr}^{-1}]$	model
EG And	70°	1.06×10^{-6}	I
	80°	9.00×10^{-7}	J
	90°	7.91×10^{-7}	K
SY Mus	80°	2.13×10^{-6}	L
	84°	1.65×10^{-6}	M
	90°	1.62×10^{-6}	N
	84°	6.51×10^{-7}	O

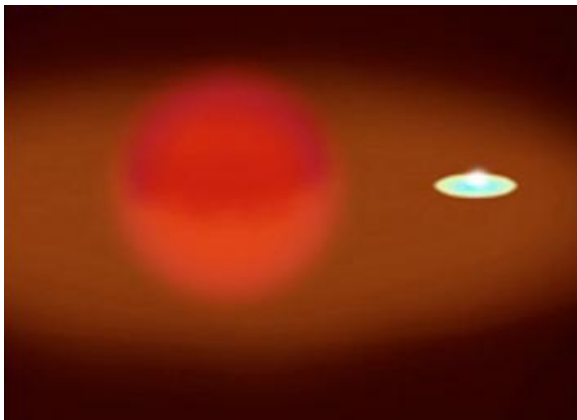
Shagatova et al. 2016, A&A 588, A83

Mass-loss rate for giants in S-type symbiotic systems from **line-of-sight independent** methods $\approx 10^{-7} M_{\odot}/\text{year}$
(from nebular emission in radio and optical wavelengths)

Seaquist et al. 1993, ApJ 410, 260

Mikołajewska et al. 2002, Adv. Space Res. 30, 2045

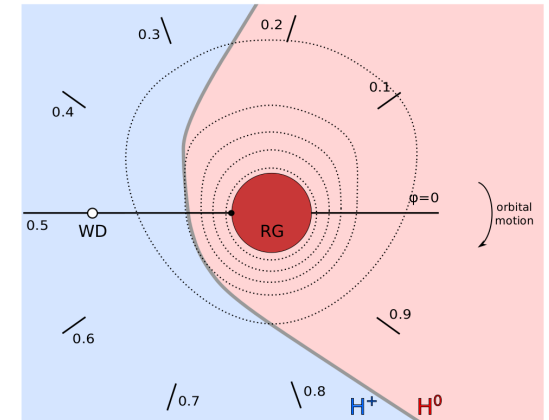
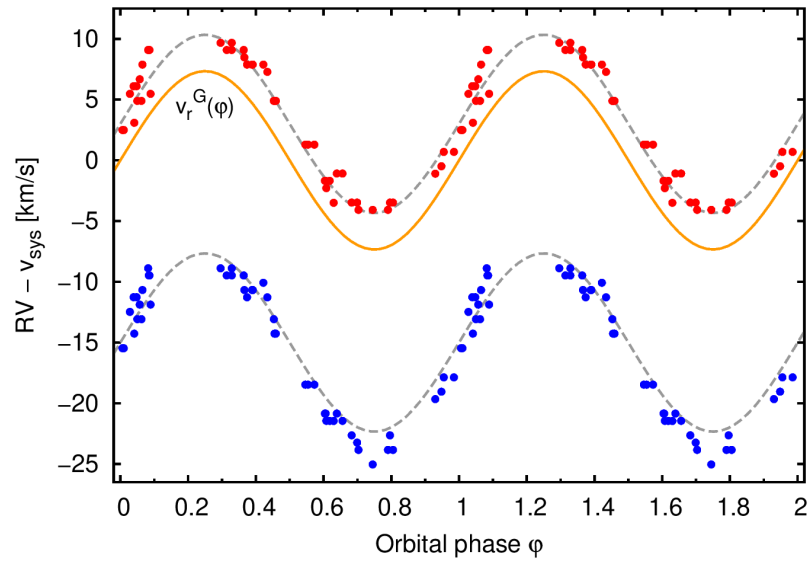
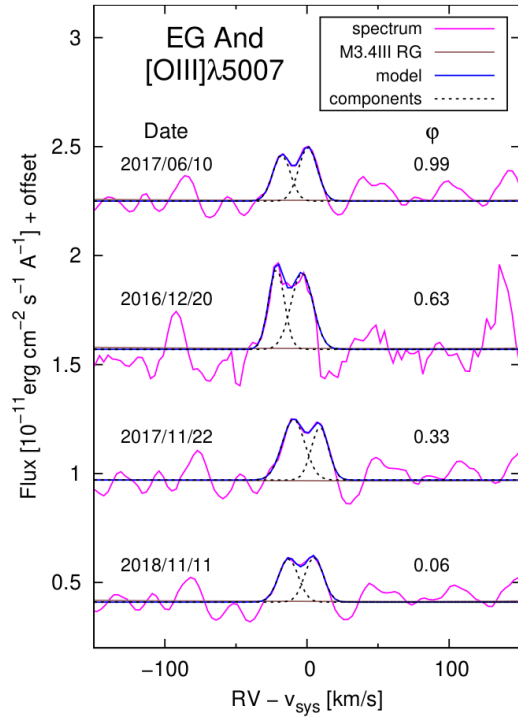
Skopal 2005, A&A 440, 995



Inconsistent with spherically symmetric wind.

Location of [OIII] $\lambda 5007$ line regions

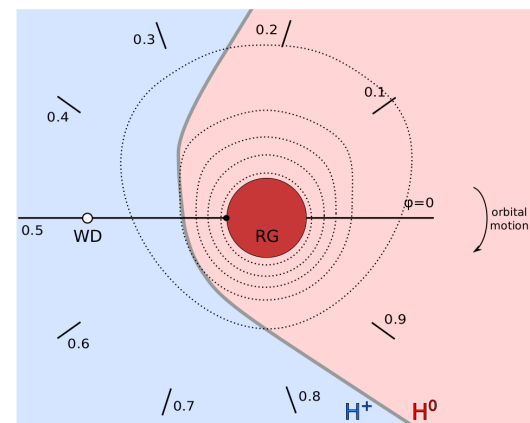
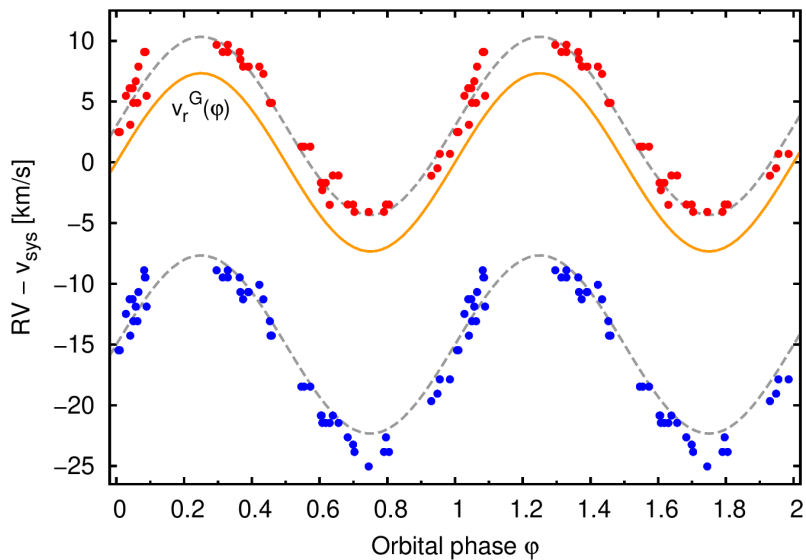
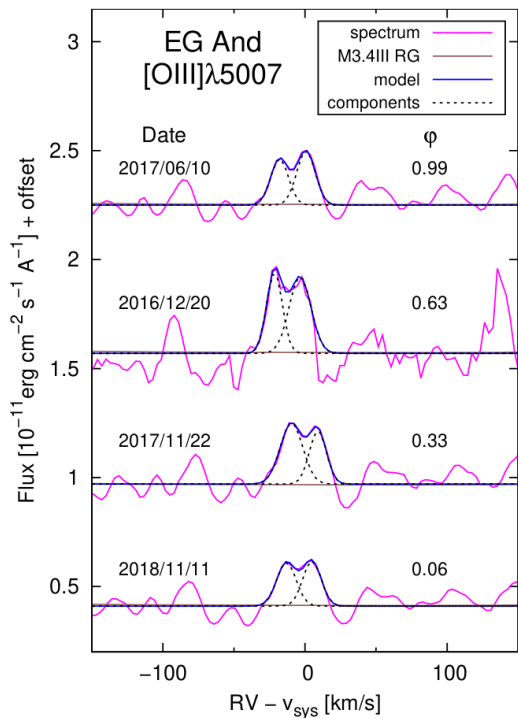
- optical spectra from 1.3m telescope at Skalnaté Pleso, $R = 30000$, $\lambda = 4200 - 7300 \text{ \AA}$



- adapted from Shagatova 2017

Location of [OIII] $\lambda 5007$ line regions

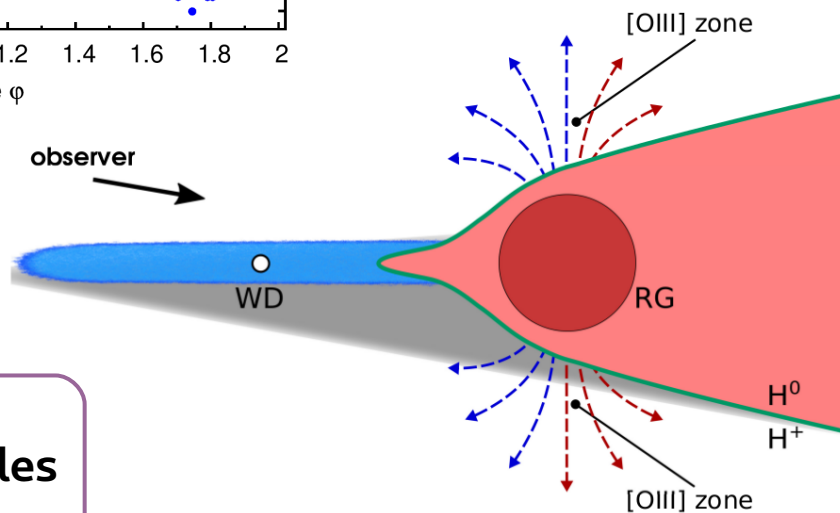
- optical spectra from 1.3m telescope at Skalnaté Pleso, $R = 30000$, $\lambda = 4200 - 7300 \text{ \AA}$




- adapted from Shagatova 2017

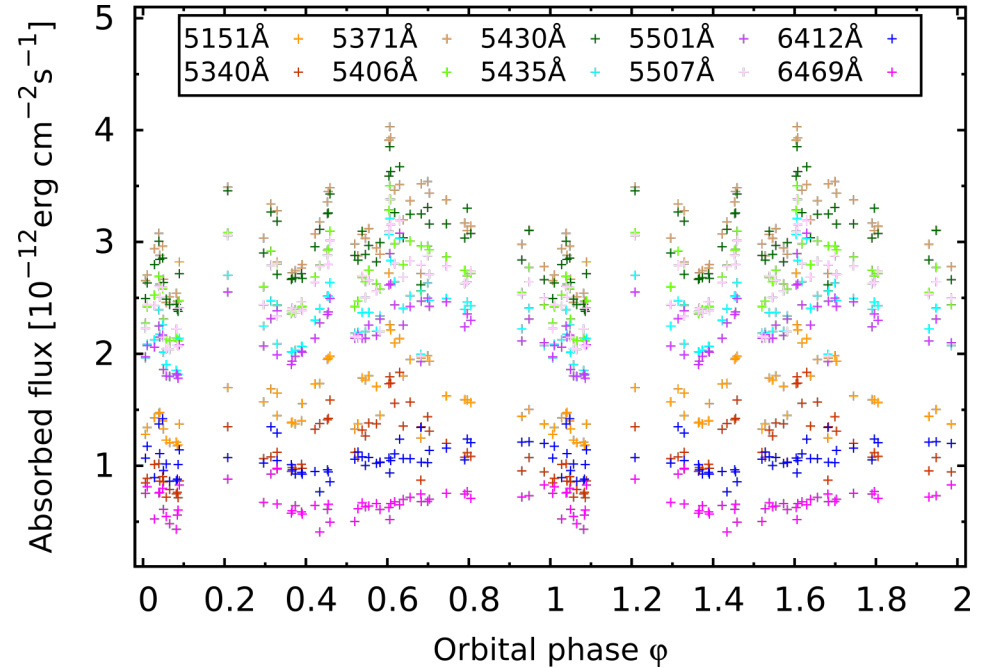
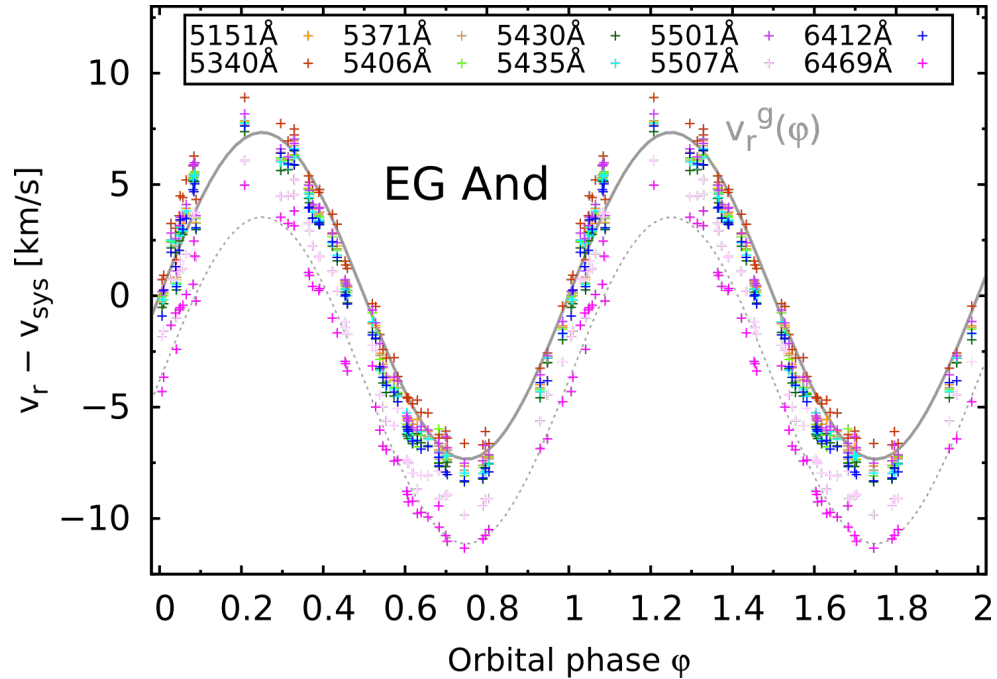
- [OIII] lines originate in regions with $n_e \sim 3 \times 10^7 \text{ cm}^{-3}$ (Skopal et al. 2001)

---> ionised **diluted wind** close to the red giant poles



 a dense material occulting fraction of the polar wind below

Orbital variability of the Fe I absorption lines



- **slow outflow** up to -5 km/s
- **inflow** values around $\phi = 0.1$

$v_r^g(\phi)$ – radial velocity of the red giant

$v_{\text{sys}} = -94.88 \text{ km s}^{-1}$ (Kenyon & Garcia 2016)

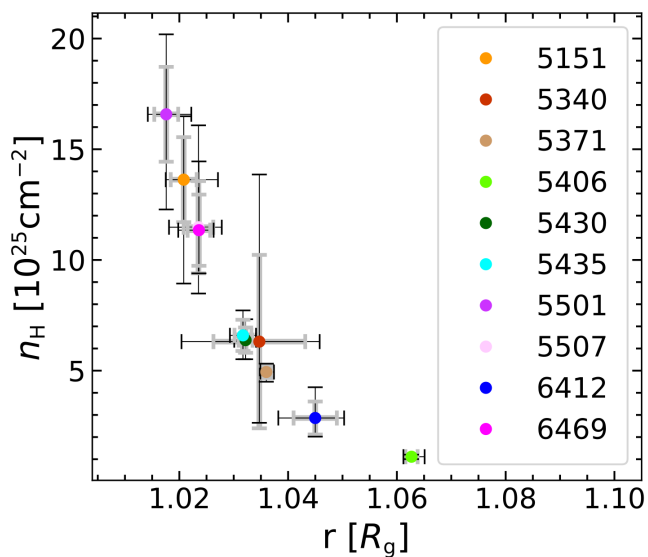
- Gaussian fits using Fityk (Wojdyr 2010)

- absorbed fluxes: maxima at $\phi \sim 0.6$

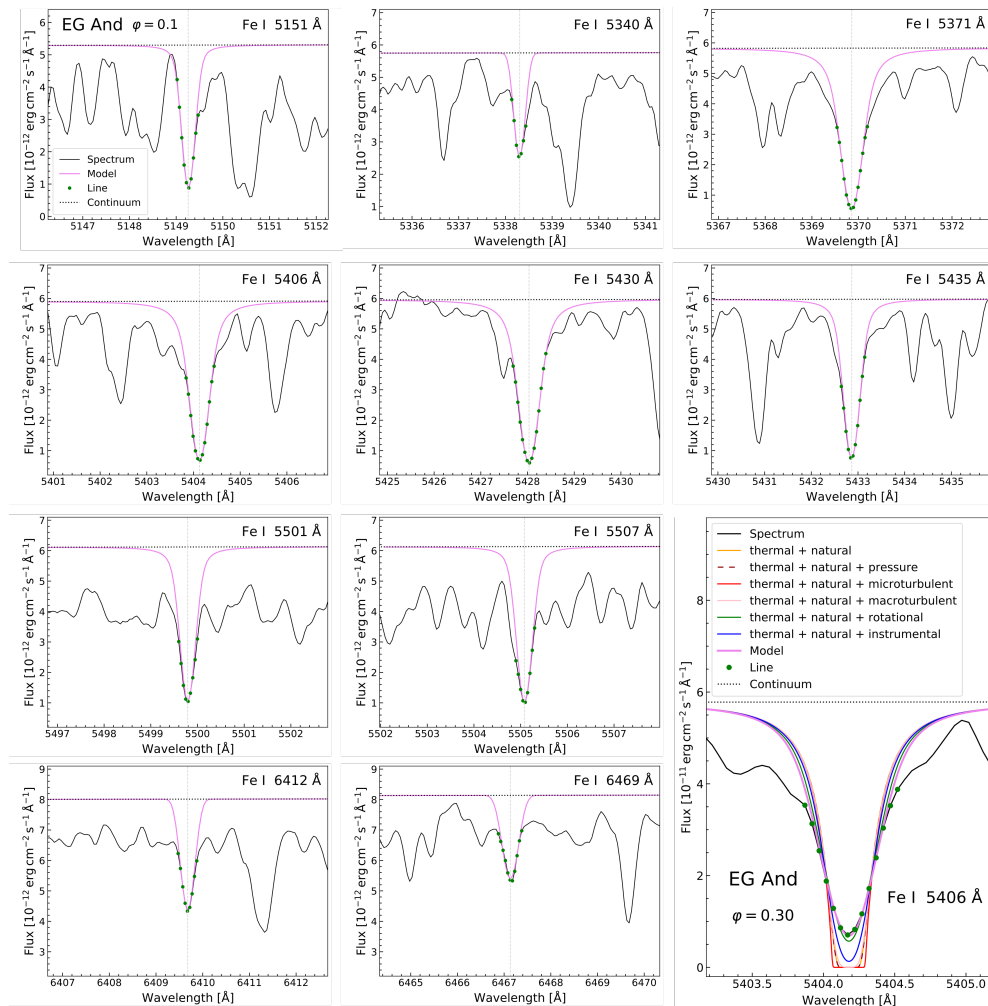
→ **asymmetry of the circumstellar matter distribution**

Modelling line profiles of Fe I absorption lines

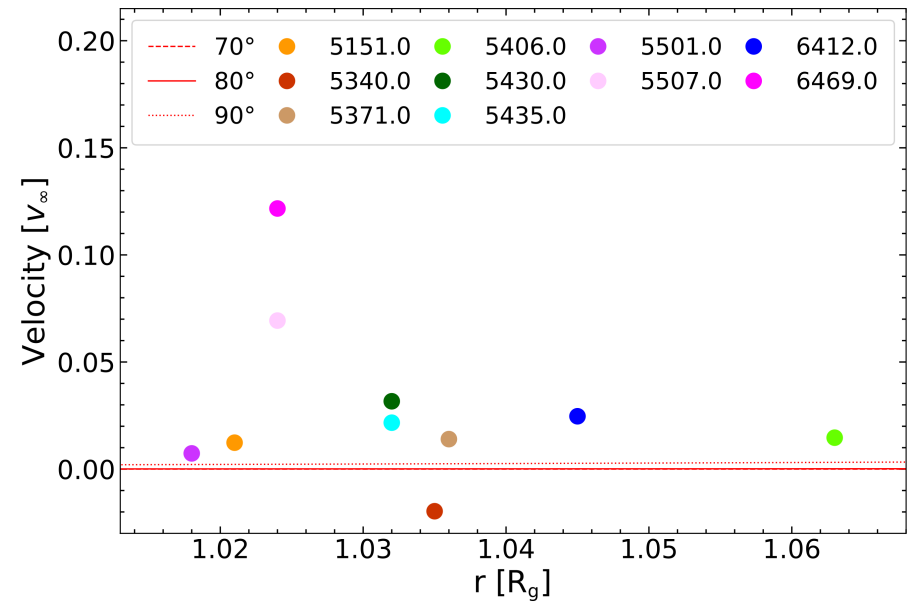
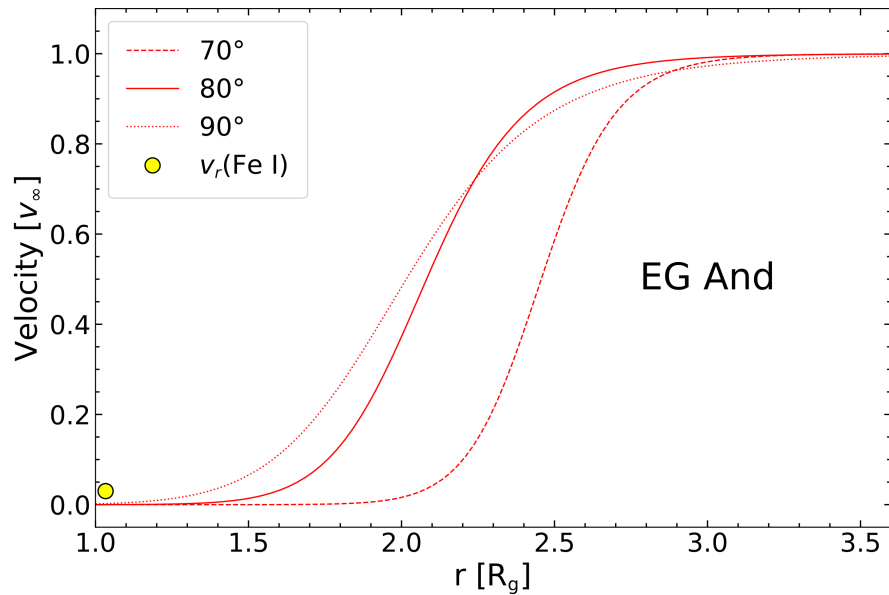
- 10 Fe I absorption lines (5151 – 6469 Å)
- 10 orbital phases
- MARCS model + extension up to $150 R_g$
- all relevant broadening mechanisms included
- atmosphere layer / **distance from center** and **radial velocity** as free parameters



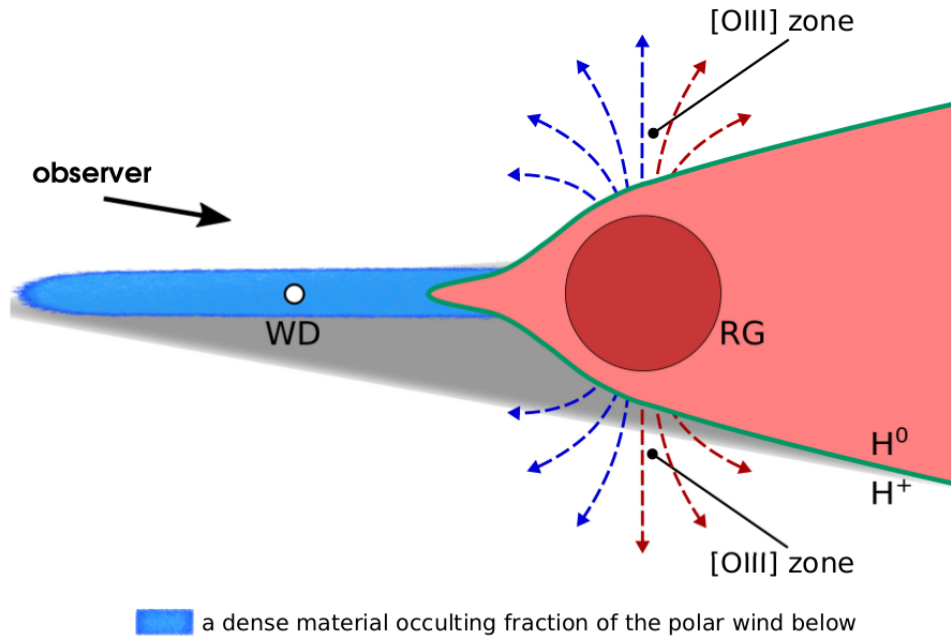
- r = deepest layer of origin of the spectral line
- heights ≈ 0.02 to $\approx 0.06 R_g$ above the R_g photosphere



Comparison with velocity profiles derived from measured near-orbital H⁰ column densities



Implications for wind focusing towards the orbital plane



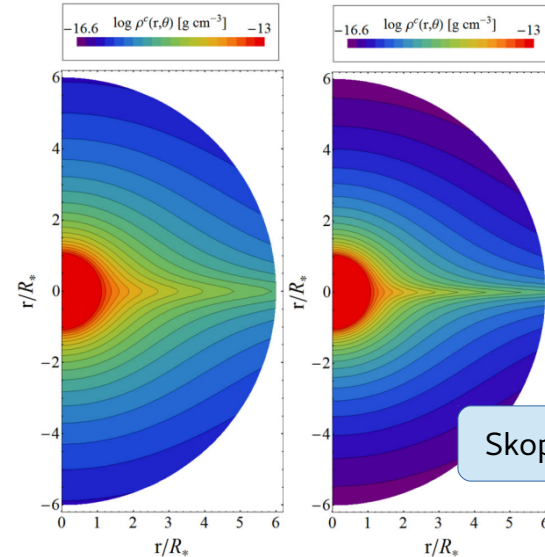
- focusing by rotation

- average over 200 modelled line profiles
- for $i = 80^\circ \pm 10^\circ$:

$$v_{\text{rot}} = 11.1_{-2.2/+2.6} \text{ km/s}$$

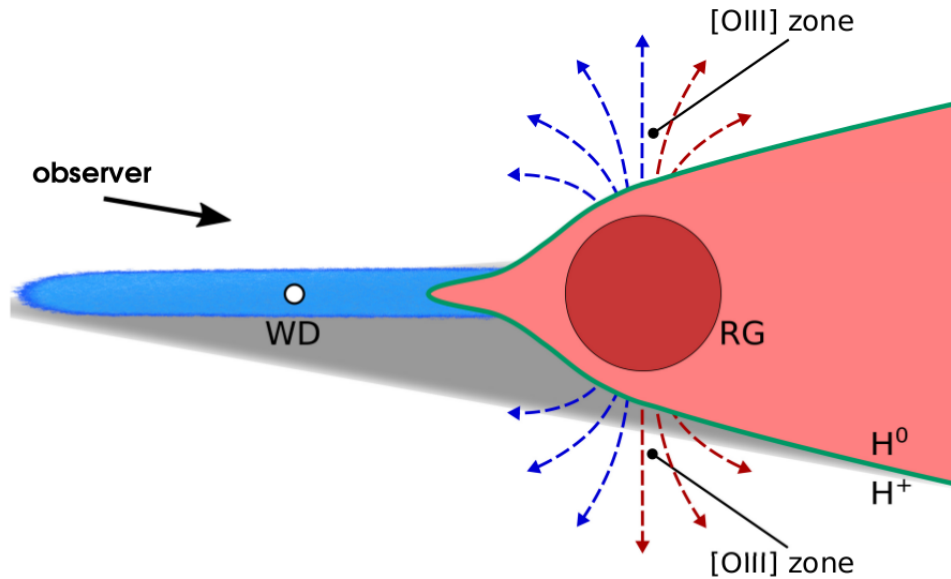
Shagatova et al. 2023


S-type systems



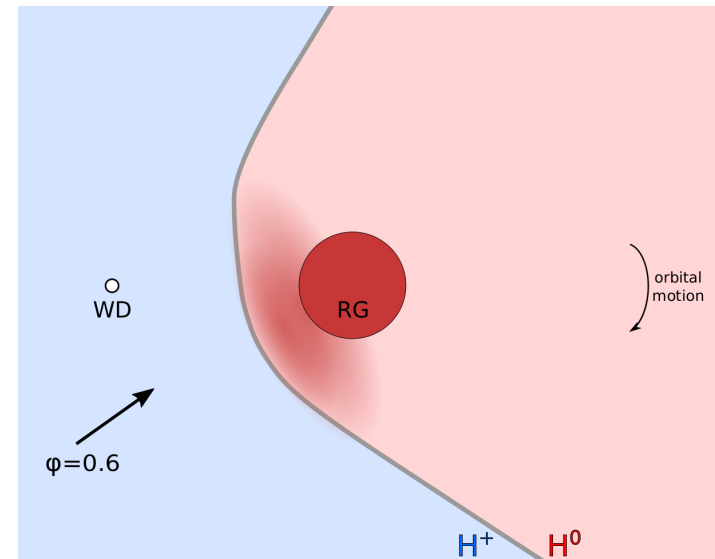
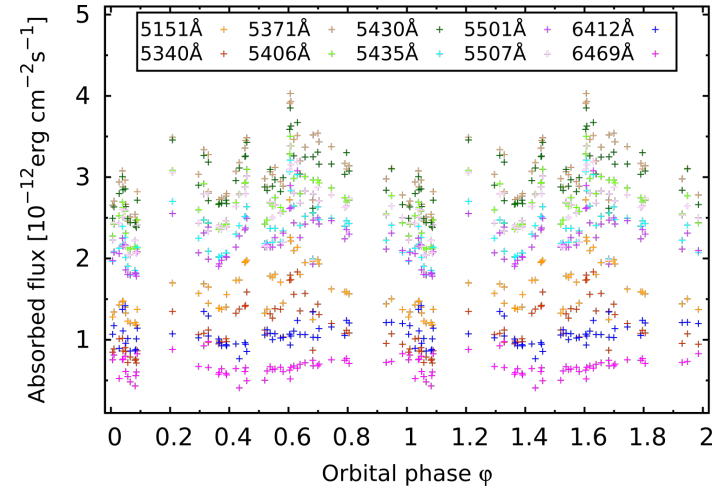
Skopal & Cariková 2015

Implications for wind focusing towards the orbital plane

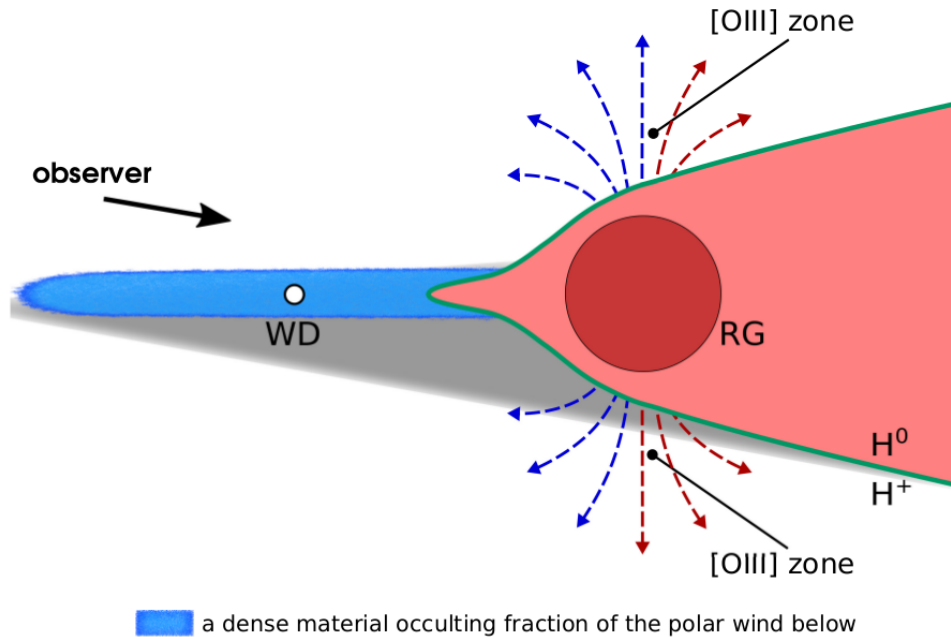


 a dense material occulting fraction of the polar wind below

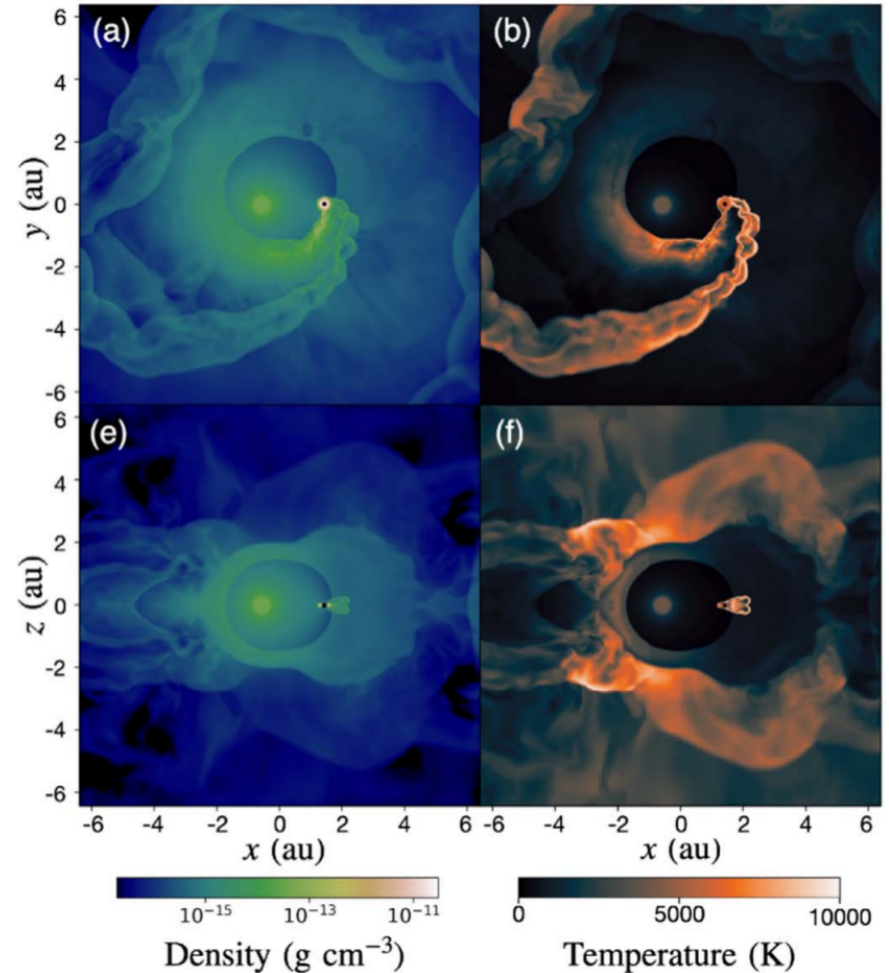
- gravitational focusing



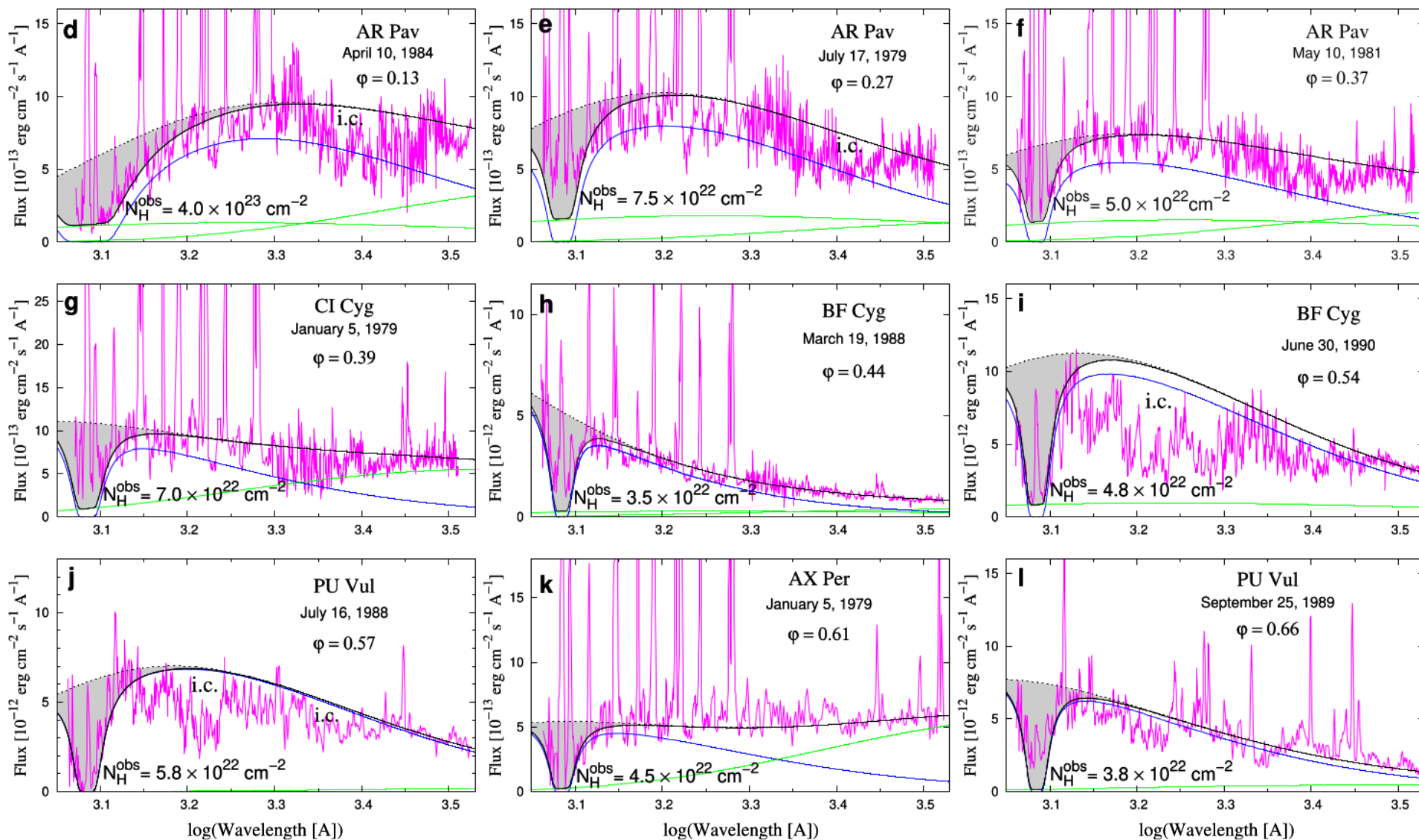
Implications for wind focusing towards the orbital plane



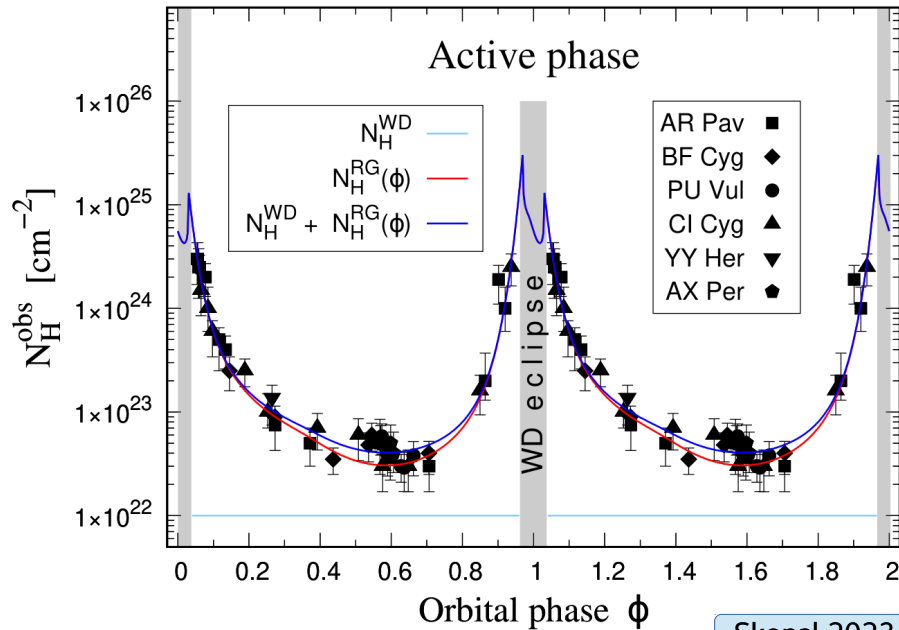
- gravitational focusing



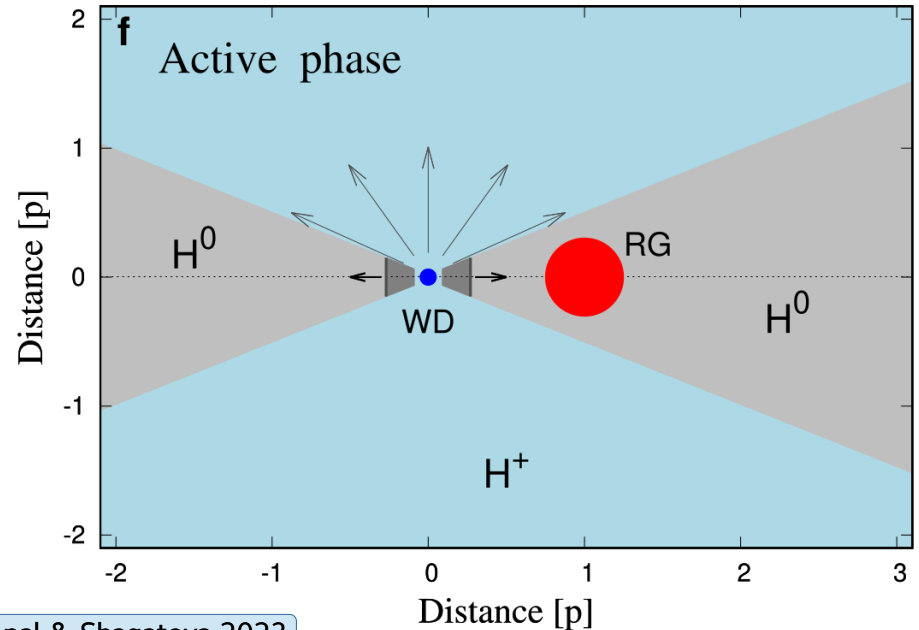
H⁰ column density during active phases



Geometry of the neutral region and mass-loss rate



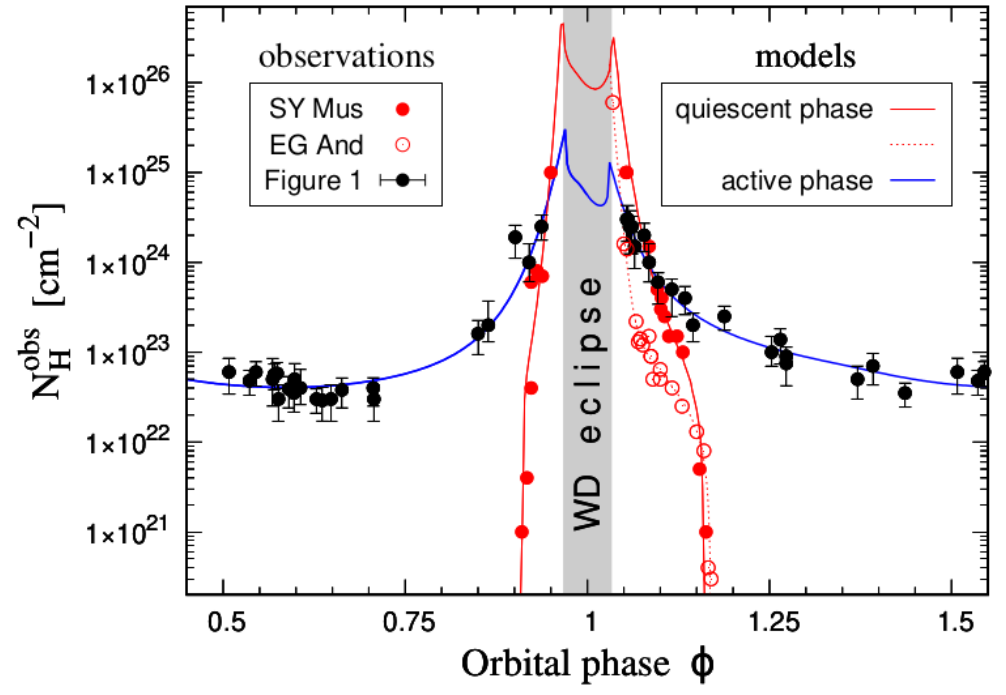
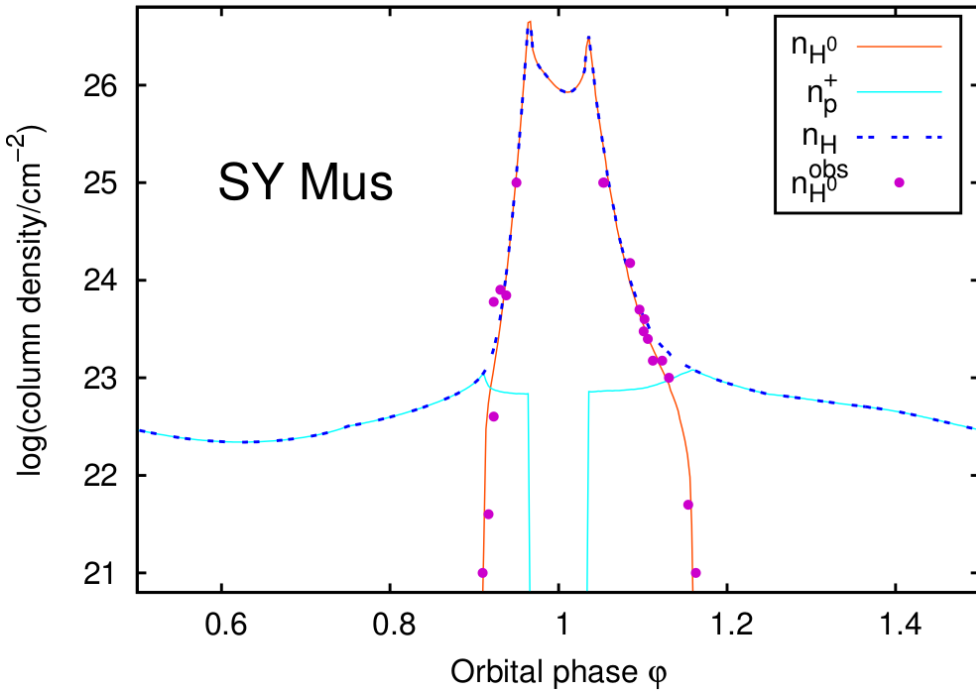
Skopal 2023, Skopal & Shagatova 2023



- transient emergence of a **neutral disk-like** structure in the orbital plane during active phases
- **dominant** contribution to n_{H} is from **red giant's wind**
- high spherical equivalent of the mass-loss rate \rightarrow **wind focusing**
 \rightarrow **effective mass transfer** onto the white dwarf companion

i	$E/I^{(a)}$	$\dot{M}_{\text{sp}}^{(b)}$
70°	E	$2.84^{+0.99}_{-1.14} \times 10^{-6}$
	I	$6.80^{+4.76}_{-3.40} \times 10^{-7}$
80°	E	$2.24^{+1.34}_{-0.78} \times 10^{-6}$
	I	$6.33^{+7.29}_{-3.65} \times 10^{-7}$
90°	E	$1.19^{+1.43}_{-0.83} \times 10^{-6}$
	I	$5.53^{+7.19}_{-4.24} \times 10^{-7}$

Wind column densities during quiescent and active phases

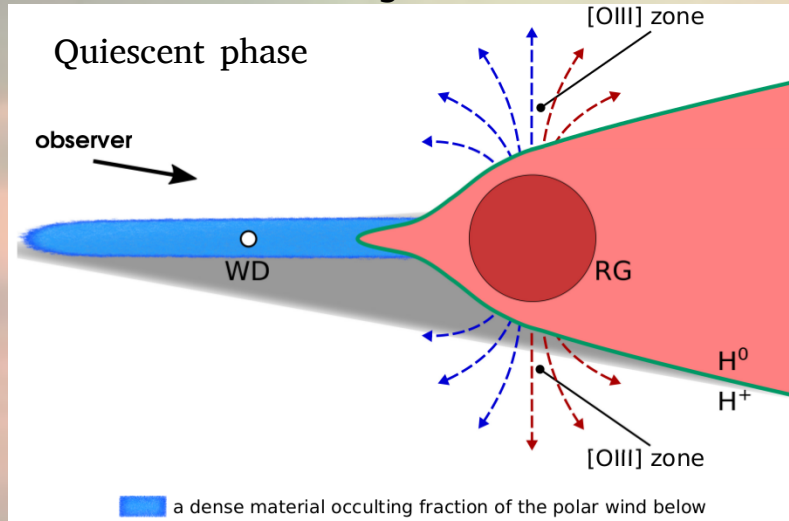


- **asymmetric distribution** of the giant's wind in the orbital plane during quiescent and active phases
- **wind focusing** towards orbital plane - a **common property** of winds from giants in S-type symbiotic stars → high luminosities of the accretors

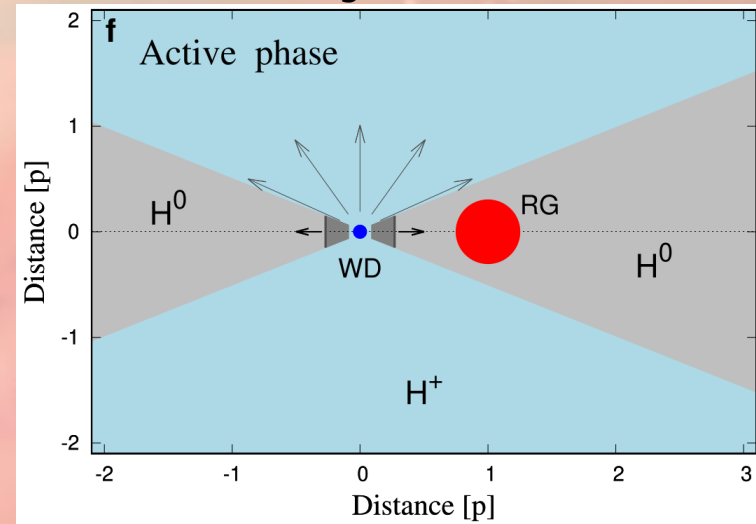
Conclusions

Wind asymmetries in S-type symbiotic stars

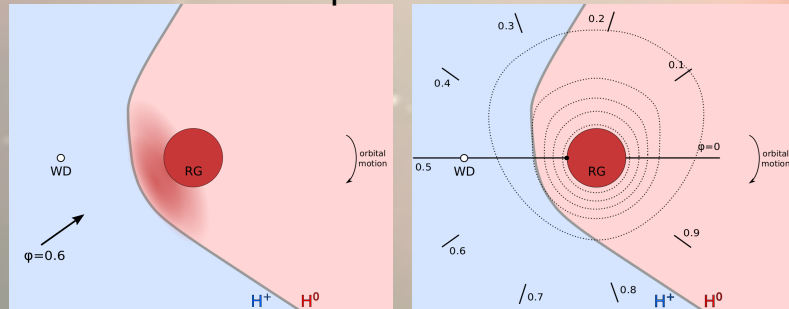
edge-on



edge-on

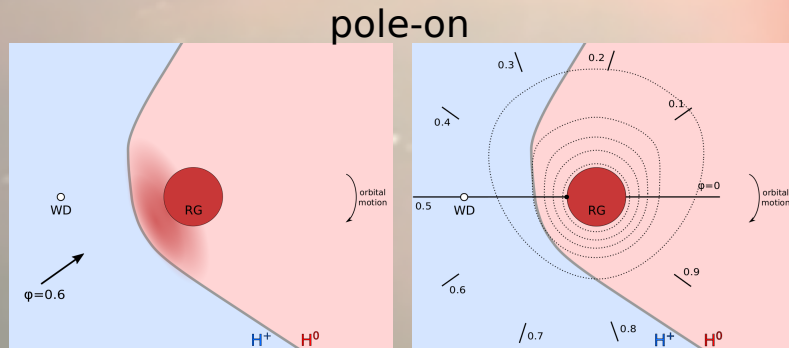
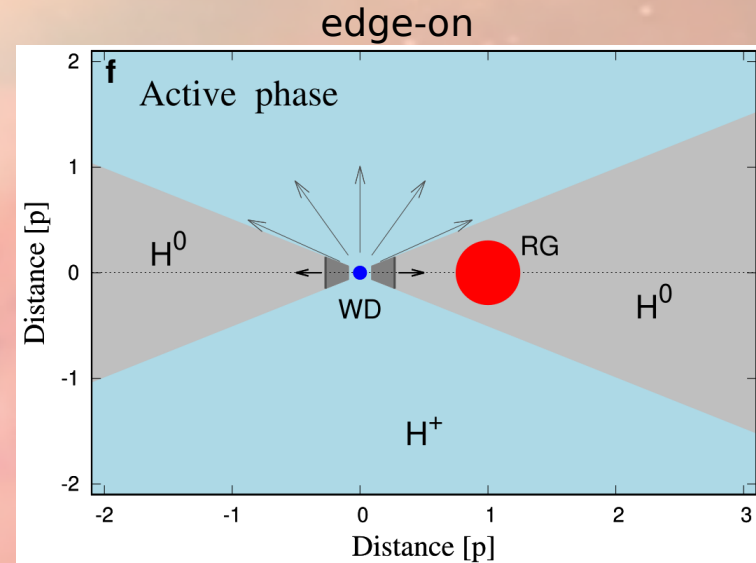
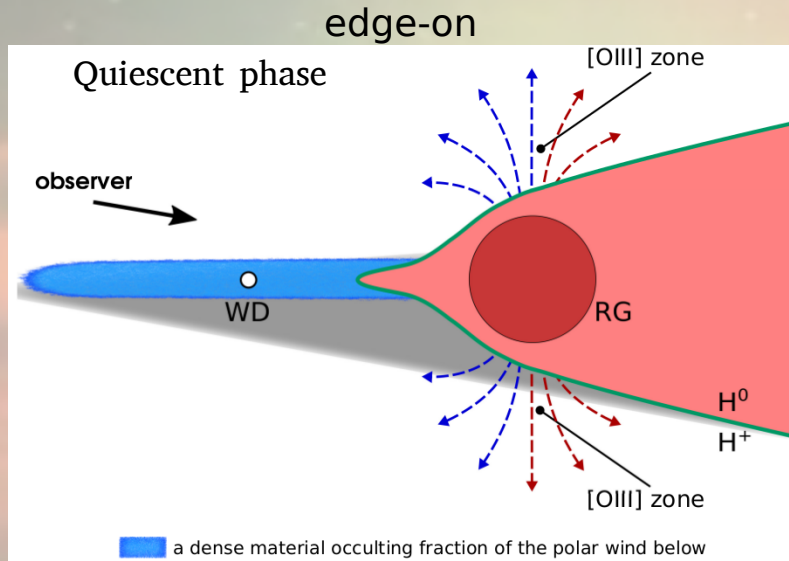


pole-on



Conclusions

Wind asymmetries in S-type symbiotic stars



Thank you for
your attention!